

Extending the piezoelectric transducer bandwidth of an optical interferometer by suppressing resonance using a high dimensional IIR filter implemented on an FPGA

Masanori Okada,^{1, a)} Takahiro Serikawa,¹ James Dannatt,^{2, b)} Masaya Kobayashi,¹ Atsushi Sakaguchi,¹ Ian Petersen,^{2, c)} and Akira Furusawa^{1, d)}

¹⁾Department of Applied Physics, School of Engineering, The University of Tokyo, 7-3-1 Hongo, Bunkyo-ku, Tokyo 113-8656, Japan.

²⁾Research School of Electrical, Energy and Materials Engineering (RSEEME), The Australian National University, Canberra 2600, Australia

(Dated: 21 April 2020)

This paper considers the application of Field Programmable Gate Array (FPGA)-based infinite impulse response (IIR) filtering to increase the usable bandwidth of a piezoelectric transducer used in optical phase locking. We experimentally perform system identification of the interferometer system with the cross-correlation method integrated on the controller hardware. Our model is then used to implement an inverse filter designed to suppress the low frequency resonant modes of the piezo-electric transducer. This filter is realized as an 24th-order IIR filter on the FPGA, while the total input-output delay is kept at 350ns. The combination of the inverse filter and the piezo-electric transducer works as a nearly-flat response position actuator, allowing us to use proportional-integral (PI) control in order to achieve stability of the closed-loop system with significant improvements over non filtered PI control. Finally, because this controller is completely digital, it is straight forward to reproduce. Our control scheme is suitable for many experiments which require highly accurate control of flexible structures.

I. INTRODUCTION

Flexible transducers are used in a wide range of experimental applications and often have highly desirable qualities. However, the control of flexible transducers can be challenging due to the existence of low frequency resonant modes present in their operating region of interest. For the transducer to be practically usable, these modes must be suppressed. Many solutions have been proposed to this end but there is no single generally accepted best solution. A common and effective solution used to address this problem is alteration of the physical structure of the transducer and its mount. By increasing the stiffness, the resonant modes may be shifted outside of the desired operating bandwidth. While effective, this solution is difficult to precisely reproduce and is only viable when the transducer may be physically modified. When the physical properties of the transducer cannot be altered we must turn to feedback control in order to achieve stabilization.

Modern feedback control techniques such as linear-quadratic-Gaussian (LQG), H_∞ and adaptive control have been applied to this problem¹⁻³, however proportional-integral (PI) control remains largely the most common technique seen in practice. This can largely be attributed to the ease of implementation and the expected disturbances to the system being largely low frequency. As a result, the more sophisticated control techniques often end up offering little discernable performance advantage. Although commonly used, the application of PI control to a piezoelectric-transducer (piezo) is far from a

trivial problem. Due to the bandwidth limitations of the piezo, the PI controller alone provides insufficient phase compensation in order to fully suppress the mechanical resonances of the piezo⁴.

Piezoelectric-transducers see wide use in many systems including but not limited to atomic force microscopes, scanning tunneling microscopes and adaptive optics. In this paper we focus our attention on their use in an optical experiment. The use of interferometers in optics experiments require precise, high-speed mechanical control of optical path lengths, while avoiding any optical loss of the signal light⁵⁻⁷. This requirement is becoming even stricter with the growing number of quantum optics experiments, where optical losses may have a huge impact on the purity of quantum states^{8,9}. The path length difference of the interferometer must be constant and accurate, meaning the path length must be stabilized against external perturbation. A common method of controlling and stabilizing the path lengths is to use the output of the interferometer and feed it back to a path length actuator. Piezoelectric transducers are typically the first choice of path length actuators in interferometer systems¹⁰⁻¹⁴ since they are considered to be virtually lossless and a dispersion-free phase modulator. Unfortunately, the low frequency mechanical resonances in the piezo-driven mirror typically limit the control bandwidth between 20-40 kHz^{15,16}. The usable bandwidth of a piezo-driven system is thus limited in practice to tens of kHz. To increase the usable bandwidth, efforts have been made to improve the frequency-response of piezo drivers¹⁷⁻¹⁹ and reduce the effect of mirror mass on the mechanical resonance^{18,20}. Now we would like another strategy: regulating the response of the piezo by signal filtering to increase the bandwidth of the PI control to offer sufficient disturbance rejection.

In this paper, we present a control scheme that introduces an infinite impulse response (IIR) filter in parallel with an integral controller in order to extend the usable bandwidth of

^{a)}okada@alice.t.u-tokyo.ac.jp

^{b)}james.dannatt@anu.edu.au

^{c)}i.r.petersen@gmail.com

^{d)}Corresponding Author : akiraf@ap.t.u-tokyo.ac.jp

a piezo while achieving the required control of an interferometer. Both the filter and controller are implemented on a field programmable gate array (FPGA). In order to systematically construct a filter that fits the piezo on each system, an integrated system identification feature is embedded on the same FPGA hardware. This results in a complete control solution. Our filter is a general-purpose linear filter with 24 programmable zeros and poles, which can cancel up to 12 mechanical resonances of a piezo. Thanks to the structure of IIR filters, the overall delay of our proposed controller is kept within 350 ns. This is a significant improvement over alternative filtering method such as Ryou et al.²¹, where a finite impulse response (FIR) filter with 25600 taps provides extreme flexibility in the frequency response, in exchange for the non-ignorable latency of 2.6 μ s. Note that the latency of the controller directly limits the available bandwidth under feedback⁴.

This paper is structured as follows: In Section II we outline our control problem of minimizing the path-length error of an interferometer system. A detailed description of the control problem is offered with a proposed solution; Section III outlines a system identification technique embedded in an FPGA used to arrive at the linear dynamic model for the interferometer system; Section IV presents a digital filter based on the obtained system model that will be used as part of our control scheme and is again embedded in the FPGA; Section V presents the experimental results after a controller is synthesised using the aforementioned filter and a Proportional-Integral control. This controller is then tested in closed-loop; Finally, we conclude in Section VI and propose future work.

The main contributions of this paper are as follows: We offer a unique control scheme that suppresses the resonant modes of a piezo while stabilizing the path-length difference of an interferometer system. The principle advantage of our scheme is that it allows for high order controllers (50th) with only 400ns delay. This makes our control scheme suited for experiments such as quantum optics with tight phase lag requirements. Our broadband control of a piezo would be also beneficial for scanning tunneling microscope or atomic force microscope experiments. Finally, by embedding a system identification module in the FPGA a complete control solution is offered.

II. PROBLEM OUTLINE : CONTROL OF A PIEZO TO STABILIZE AN OPTICAL INTERFEROMETER

The following section outlines the feedback control problem of designing a controller that provides accurate optical phase locking of a Mach-Zehnder interferometer when used in an optics experiment. Due to the nano-second latency and large bandwidth of our proposed scheme we will consider requirements that render this control scheme suitable for quantum optics experiments. Thus the requirement for accuracy in locking we will consider is far stricter than what might be expected in classical light experiments. We will structure this section as follows: First we offer a full system description; Our control problem is then outlined; Finally we introduce a dual filter and PI controller implemented on an FPGA that solves

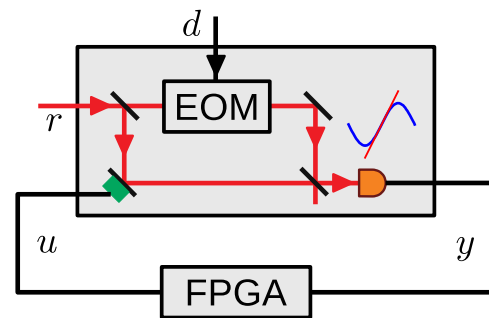


FIG. 1. Closed-loop system with Mach-Zehnder interferometer and FPGA controller. Where r is the 860 nm laser input to the interferometer, y is the measured output of the detector and u is the control input to the piezo, d is the artificial noise added by electro-optic modulator (EOM).

this problem.

A. System Description

Consider the feedback loop of an optical interferometer and digital controller shown in Fig (1). This system is comprised of a Mach-Zehnder interferometer with 860 nm laser input (r) and a RedPitaya signal processing board acting as a digital controller. The RedPitaya features a ZYNQ-7010 FPGA-chip, and analog-to-digital converter (ADC) and digital-to-analog converter (DAC), both of which are driven by a 125 MHz-clock, and 80 pieces of DSP48E1 multiplier-accumulator (MACC) cores. Shown in Fig (1), an artificial phase noise d is added to the interferometer by an electro-optic modulator (EOM) on the one side of the arm, which is to be canceled by the piezo-actuator on the other arm. We then evaluate the performance of the controller. The two outputs of the beam-splitter shown in Fig (1) go to a second 50:50 beam-splitter, and are then detected by photo detectors. One of the outputs of the photo detectors is used for the phase control, while the other is used for the verification of the system. The output of the photo detector is denoted as y and corresponds to the path length difference of the two arms of the interferometer. This value is derived from the phase signal θ as $y \propto \sin\theta$. This is then linearized as $y \propto \theta$ for small deviations. Finally, u corresponds to our control input to the piezo.

In order to describe our control problem we will represent the system shown in Fig (1) with the block diagram shown in Fig (2). Here, $G(s)$ and $C(s)$ denote the transfer function of our plant to be controlled and of our digital controller, respectively. d represents the noise sources which disturbs interferometer's path length such as DAC's noise, VGA's noise (before PZT) and mirror's vibration for example. k is an adjustable gain parameter, offset determines the control point, and F is the IIR filter to be developed and is followed by 1st order low-pass filter. Finally, the integral control can be observed on the lower parallel branch. The motivation for this scheme is that as DC gains are pushed to the lower integral branch, the mean value of the upper branch can be controlled around DC. This allows

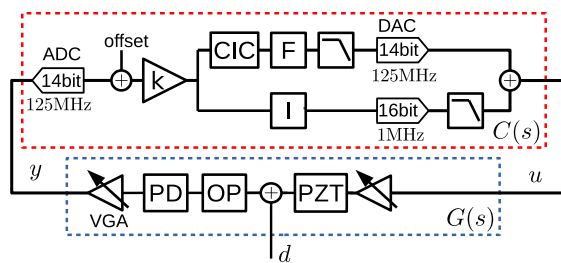


FIG. 2. Block diagram of the closed-loop system. OP is the system optics, PD is a photo detector, PZT is the piezo, and VGA is a variable gain amplifier. Dotted area labeled by $G(s)$ represents the interferometer and associated amplifiers that by $C(s)$ is our digital controller implemented on an FPGA. F is an IIR filter followed by 1st order low-pass filter and CIC is a cascaded integrator-comb decimation filter.

us to leverage the maximum dynamic range of the IIR filter F .

B. The control problem

Consider the closed loop system shown in Fig (2). We are concerned with the control problem of generating a feedback controller $C(s)$ that minimizes the path length difference of interferometer while being robust to external disturbances. As discussed in the introduction, the complexity of this control problem lies in the resonant modes of the piezo being present in our operating frequency range, limiting the usable gain of a PI controller. Thus, our interest is in how controller gain can be increased while minimizing the sensitivity function

$$S = \frac{y}{d} = \frac{1}{1 + C(s)G(s)}. \quad (1)$$

This function describes how the disturbance d to the interferometer's path difference y is suppressed by a feedback controller $C(s)$.

A typical frequency response model of a piezo is shown in Fig (3). Of particular interest are the two resonances at several tens of kHz and a roll-off at 100 kHz. These may be attributed to acoustic resonances of the piezo's volume, mechanical resonances of the mounting back-masses and the second order roll-off of the mirror's mass¹⁹. These resonances are expressed by a pair of second order zeros and poles, which can make the feedback loop of Fig (2) unstable. Intuitively, this is because the sharp phase lags shown in Fig (3) contribute to the feedback phase. This can cause the system to start oscillating, when the total phase lag reaches 180 deg within the frequency band that the controller gain is larger than 1¹⁹.

The impact of the aforementioned resonance on the system is that it limits the usable controller gain and directly impacts the error in path difference that can be achieved. With an I controller $C(s) = k_I/s$, which have 90 degrees of phase lag, the possible maximum gain k_I is limited by the condition that $|G(s)k_I/s| < 1$ where the phase delay of the plant gain $G(s)$ is

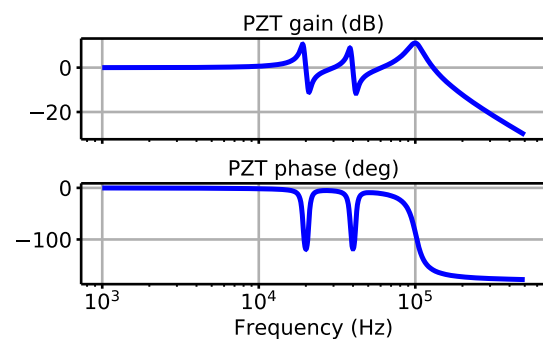


FIG. 3. Frequency response of a typical piezo-driven mirror.

larger than 90 degrees. Resonances that lie at lower frequency imposes more serious limitation on k_I . Hence our control problem becomes how do we increase the controllable (i.e. free from the lag of mechanical resonances) bandwidth of the actuator.

C. Control design and feedback strategy

In order to increase the usable bandwidth of our interferometer system we will adopt a dual filtering/control approach. As shown in Fig (2), our proposed controller can be considered as two parallel sub controllers. The lower branch is the integral control required for stabilization. We use an integral controller as the external system noise d typically comes from mechanical vibration, we can safely assume its power spectrum is concentrated around DC. The upper branch consists of a filter F that will be used to shape the frequency response of the closed loop system. Our control problem is then how to create a filter that cancels the resonant modes of the piezo and maximises the closed-loop bandwidth, in order to increase the performance of the integral control and minimize the sensitivity in (1). To this end we opted to use a canceling filter with the form $F = 1/G(s)$. This filter's zeros and poles are derived from the system poles and zeros respectively. We expect this canceling (or inverse) filter will cancel out the resonant peaks in the frequency response of the system resulting in a flat frequency response. However in practice, ideal cancellation is not possible. The measured transfer function of the piezo suggests it is non-minimum phase and therefore has unstable zeros. This is significant because any unstable zeros can not be stabilized by the inverse filter as they become unstable poles (one relevant example of an unstable zero is the Pade approximation of the time-lag²²).

III. SYSTEM IDENTIFICATION

In order to synthesize a filter $F = 1/G(s)$ we require a model of $G(s)$. We now discuss the system identification process used to obtain the model of our system. We obtain the frequency response $G(s)$ using the White-Noise method of system identification²³. This method was chosen for its

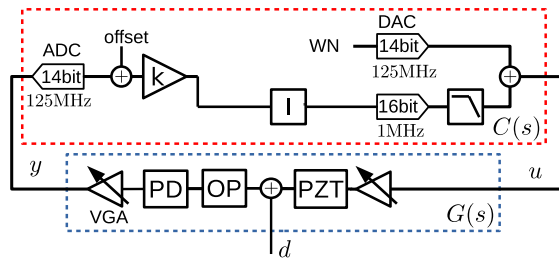


FIG. 4. Controller configuration used to perform system identification. WN is white noise signal implemented by M-sequence. White noise is added from the upper branch of the circuit and the response is measured. The control point is stabilized with integral control during the measurement.

effectiveness under the assumption of linearity of the system. The goal of system identification here is to establish a function that characterises the systems zeros and poles. This section is presented in two parts; Firstly we discuss our choice of system identification method and how it may be implemented on an FPGA; We then analyse the implemented method and compare the result with a frequency response obtained using a commercial network analyser.

A. System identification options

For a single system, perhaps the simplest way to perform system identification is to take a frequency response measurement of the system using a network analyzer. In practice however, a system may not always be available during operation for measurement or the number of measurements required prohibits this method. In the field of quantum optics for example, it is usual to need to lock tens of interferometers and identify them. Also, the frequency response of the piezo in the interferometer is sensitive to external parameters such as temperature and is therefore changing over time. System identification must be repeated often and for each interferometer in order to minimize the path error. Considering this, an alternative to an external network analyser is needed.

Our solution is to implement the system identification process on-board the FPGA housing our controller. The data from these controllers can then be sent to a single personal computer (PC) and the frequency response of each piezo is calculated. In order to realize this, the digital controller is configured as in Fig (4), where WN is an M-sequence white noise signal. M-sequence was chosen over other methods after considering its ease of implementation in an FPGA due to being composed of only shift-registers and basic logic circuits. Also, note the continued presence of the integral control. This is necessary so the system is stabilized around the control point during the frequency response measurement.

Our approach will be to obtain the impulse response of the system in the above configuration, and thereby calculate the frequency response via Fourier transform. In our white noise approach the discrete-time impulse response $h(k)$ of the target system is given as the cross-correlation of the input white

noise $u(k)$ and output $y(k)$. The white noise signal $u(k)$ can be characterized by the auto-correlation as

$$\sum_k u(k)u(k-m) = 1 \text{ if } m = 0 \text{ else } 0, \quad (2)$$

where the variance of the white noise is normalized as 1. The output signal sampled by the ADC is

$$y(k) = \sum_m^N h(m)u(k-m). \quad (3)$$

The sampled output signal $y(k)$ and white noise input $u(k)$ are then sent to an external PC, where their cross correlation is computed, giving the impulse response of the system as

$$h(k) = \sum_m y(m)u(m-k). \quad (4)$$

The Fourier transform is then used to obtain the frequency response $H(z)$ of the system, which is equal to

$$H(z) = \frac{G(z)}{1 - \frac{G(z)k_i}{z}}, \quad (5)$$

where k_i is the integrator gain value in the controller. We choose k_i as small as possible such that $H(z)$ can be approximated to $G(z)$ while linearity of the interferometer output is maintained.

B. Implementation

The aforementioned system identification process was coded on the RedPitaya FPGA. We will now discuss the results of running this system identification process on a piezo. Fig (5) shows the measured frequency response of the system shown in Fig (1). In Fig (5), the results from our system identification process are compared with the frequency response obtained using a Keysight E5061B network analyzer. 4000000 samples of M-sequence and its output is taken by 5MHz of sampling rate. Because the smallest linewidth of the mechanical structure is expected to be around 1kHz, 4000000 samples of data are divided into 200 sets, averaging 200 of cross-correlation to get the impulse response of the system, where we can get 250Hz of resolution bandwidth. Blue line shown in Fig (1) is the Fourier Transform of this impulse response. We can clearly see strong agreement between the two traces. It takes 0.8s to finish the data sampling itself with these parameters. Considering another processes such as communication between RedPitaya and external PC or numerical calculation, the total time for system identification is about 10 seconds.

Our system identification process returns the frequency response $H(z)$ corresponding to the closed-loop transfer function (5). We then rearrange this for $G(s)$. This new frequency response is then fitted by the least-square method which includes twelve stable zeros and poles at maximum and also an auxiliary time-lag as fitting parameters. The frequency response shown in Fig(5) is fitted by seven poles, six zeros and $1.2\mu\text{s}$

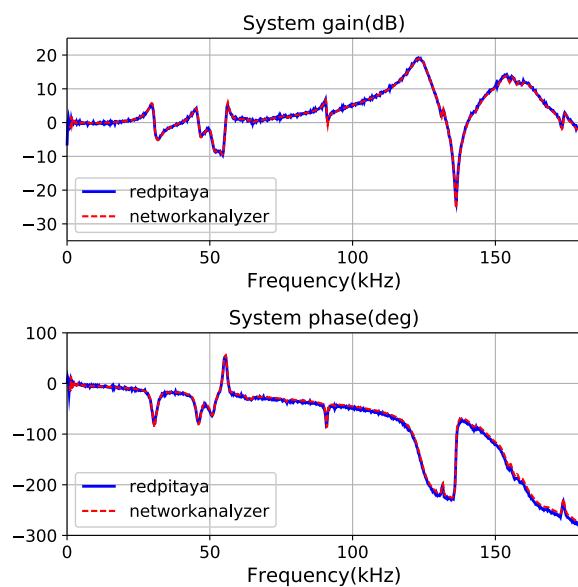


FIG. 5. Measured frequency response of the system $G(s)$ under PI stabilization. Blue line shows frequency response measured by our RedPitaya controller. Red line is the frequency response measured by a commercial network analyzer.

of time lag. The poles and zeroes of this model then form the respective zeroes and poles of an inverse filter $F \approx 1/G(s)$, while we ignore the time-lag. In the following section we discuss the design and implementation of this filter.

IV. DIGITAL FILTER DESIGN

The following section discusses the digital implementation of the inverse filter $F \approx 1/G(s)$. This filter is designed in order to shape the frequency response of the plant in an effort to cancel the resonant modes of the piezo and extend the system's usable bandwidth. When considering digital filters we either use a non-recursive or a recursive filter. We will consider these in the form of the finite impulse response and the infinite impulse response filters respectively.

This section will be structured as follows; We first discuss the available options for digital filtering and the motivation for our choice of filter; We then discuss the design of an IIR filter that meets our design requirements; Finally, we discuss the implementation of this filter and its impact on our closed-loop system.

A. FIR Filter

An FIR filter is the direct implementation of the convolution of the impulse response $y(n) = \sum_k^N h(k)x(n-k)$. In the case of the FIR filter, frequency resolution is directly proportional to tap number N . This makes the FIR filter more accurate but slower and higher order than the equivalent IIR filter. In the implementation in [21], an FIR filter on RedPitaya composed

of $N = 25600$ taps is used to cancel the mechanical structure of a piezo in an optical cavity. To implement such a large number of taps, MACC operations are repeatedly used to obtain an output, resulting in $2.6\mu s$ of time lag. In contrast to this, an IIR filter only needs a number of taps proportional to the dimension of the mechanical system model. This drastically reduces the number of operations required for a comparable frequency resolution. However this also comes with stability and error issues which cannot be ignored.

B. IIR Filter

An ideal IIR filter can be modelled as follows. The output y is given by

$$y(n) = \sum_k a_k x(n-k) + \sum_k b_k y(n-k), \quad (6)$$

An impulse invariant transform $z = e^{sdt}$ is used to set the filter coefficients a_k, b_k . This relationship is then approximated to

$$z_{re} + iz_{im} \approx 1 + 2\pi s_{im} dt, \quad (7)$$

where both real part and imaginary part of the s are assumed to be much larger than the sampling rate i.e. $s_{re}, s_{im} \gg 1/dt$.

Implementing IIR filters requires careful analysis of the accuracy of the coefficients and internal signal²⁴, especially when using fixed point encoding which can be efficiently realized in FPGAs. In order to ensure the integrity of our filter, there are two major errors we need to consider: Firstly, truncation errors ϵ_i in the coefficients of a_i that changes the corresponding poles $p_i \rightarrow p_i + \epsilon_i$. This can result in an undesirable frequency shift of the transfer function. Secondly, truncation errors in the multipliers are accumulated in the signal giving rise to an offset error. Since the hardware resource is limited by the requirements of the latency and the cost, our objective is to make the bit-width of the fixed-point signals as small as possible. An analysis of quantization noise and truncation errors pertaining to our system can be found in Appendix A and B respectively. As we will discuss in the following section, these sources of errors can be mitigated in our implementation and therefore the speed advantage of the IIR filter makes it a more suitable candidate for our application than the FIR filter.

C. IIR inverse filter Design

In this section we will discuss the design of a digital IIR filter acting as an inverse filter. The requirements for this filter are that it approximates the inverse of our plant $G(s)$ as closely as possible while minimizing the errors outlined in the previous subsection.

Fig (6) shows the configuration of the IIR filter to be implemented as our digital filter. The configuration is made up of 12 2nd order IIR filters split into three groups of four filters. This creates a 24th order filter as in Fig (7). Here each filter module processes a single signal four times. The filter-coefficients and the internal resistors are switched sequentially

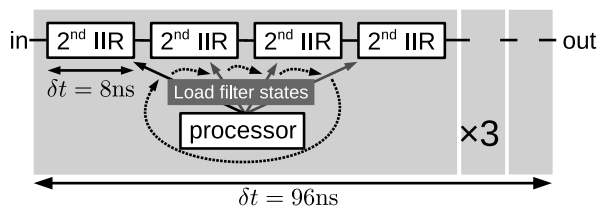


FIG. 6. Block diagram of 24th order IIR filter.

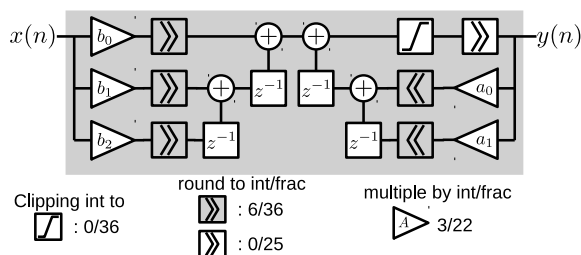


FIG. 7. Hardware implementation of one 2nd order IIR filter.

each cycle. This structure is chosen in order to maximise our available frequency resolution and reduces the amount of required MACC operations. However, this increase in resolution comes at the expense of reducing the processing rate by 1/4. This rate can be increased or decreased depending on the latency requirements of the system. The signal is re-sampled at 31.25MHz using cascaded integrator-comb filter (CIC) prior to the inverse filter to match this new processing rate. Note that, except for the latency of the CIC filter, there is no extra time lag that arises from the re-sampling because each step of 2nd order IIR filters results in one clock delay at the 125MHz operating clock. Although a choice of 24th order is made here, it is not unique. A higher dimensional filter further expands the feedback gain and in principle it is only limited by the time lag of the controller. There is a trade-off between the order of the controller and the latency of the inverse filter, which should be optimized depending on the unique system and the hardware limitations.

We now discuss the implementation of each individual 2nd order IIR filter.

In order to keep accuracy of our inverse filter, we need to choose a number of bits by which each filter coefficient will be represented. The effect of quantization error is discussed in detail in Appendix A. with the outcome being that in order to keep the accuracy we must satisfy the criteria $\Delta z/z \leq 0.01$. Thus the fractional bit number b is set to 22 in order to satisfy this. Three more bits are then used to implement the integral component of the coefficients. Thus, in total 25 bits are used for implementing each filter coefficient. This number is reasonable as it is the upper limit of what can be efficiently processed by the input to the MACC on this FPGA.

We now choose a number of bits larger than 25 for the internal signals of the IIR filter to keep the accumulating rounding error small enough. We opted to use 36 bits here as it was the smallest number greater than 25 that could efficiently pro-

cessed by our MACCs. This number means that the maximum value of the accumulated rounding error is calculated to 20 bits. This then leaves 16 bits that can be considered as error free signal. Multiplication of the 36 bit signal and 25 bit coefficients is achieved using the single instruction multiple data (SIMD) method using two *DSP48E1* elements (See [25]). After each multiplication operation, fractional bits are rounded to 36 bits again. At the output of the filter, the integral components are clipped and fractional bits are rounded to 25 bits to match the next 2nd-IIR filter cord length. Each filter takes exactly 1-clock cycle to process the input which means we need only one MACC operation in the critical path.

The time lag of each 2nd order IIR filter module is 8ns. With 4 modules in each segment and a total of 3 segments, in total the delay of the filter F is 96ns. The breakdown of the overall latency of 350ns is shown in Table 1. The cascaded IIR filter and decimation filter has 136ns of delay when the extra delay of the 3 clock of the CIC filter and 1 clock of a synchronization flip-flop at the output is taken into account. The delay from the input to FPGA to the input of the plant $G(s)$ without the filter is measured as 254ns

TABLE I. Delay components of our controller.

	Lag (ns)	Lag (clocks)
ADC pipeline delay	56	7
DAC latency	24	3
IIR inverse filter	104	12 + 1
CIC filter	32	3 + 1
Other logic elements in the FPGA	38	?
Analog frontend	96	

V. EXPERIMENTAL RESULTS

We will now discuss the aforementioned filter after implementation in the FPGA as part of the digital controller.

Fig (8) shows the frequency response of the plant $G(s)$, the cascaded IIR filter (inverse filter), and the cascade of the plant $G(s)$ and inverse filter. Blue line corresponds to the measured frequency response of the system $G(s)$ under integral control as in Fig (4). The frequency response of the inverse filter is shown by red line, which is measured by a commercial network analyzer. The result of cascading plant $G(s)$ and the inverse filter is shown by green line. If the plant has no unstable-zero and all poles and zeros are cancelled by the inverse filter, green line gives flat curves in both gain and phase response. In the gain curve, we see the response is flattened by the inverse filter, suggesting the inverse filter accurately captures the shape of the inverse of the $G(s)$. The phase curve is clearly offset from the 0 degree, however. The offset from the ideally cancelled phase response is attributed to the non-minimum phase components, which has unstable-zeros and so can not be cancelled by inverse filter. The following three factors contribute to the phase offset in Fig(8): Firstly, non-minimum phase component of the piezo system, which is equivalent to $1.2\mu s$ of time lag in the frequency region we are interested

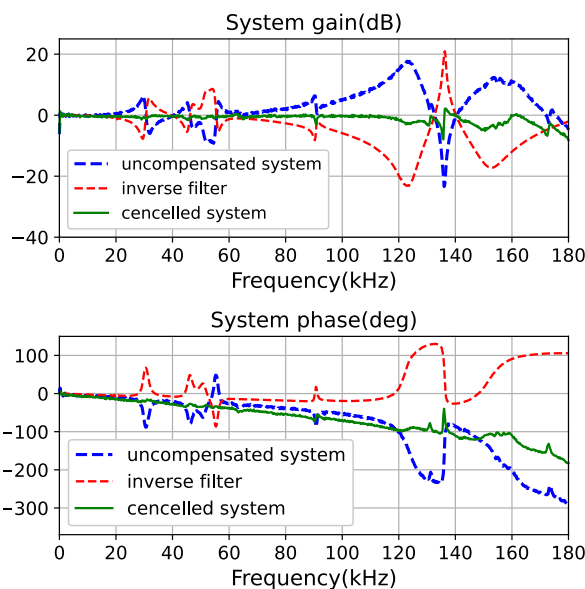


FIG. 8. Frequency response of the plant (blue), inverse filter (red), and the cascade of these two systems (green).

in. We emphasize that this time-lag component does not come from our controller but the plant. Secondly, 350ns delay of the RedPitaya controller. And finally, 300kHz 2nd order low-pass filter cascaded to the inverse filter. This low-pass filter is introduced because the estimated zeros-poles model has roll-off at 150kHz and six pair of zeros and poles. The inverse of this model has an increasing gain at high frequency, which possibly saturates the cascaded IIR filter. To guarantee the stability of the inverse filter, we cascaded the 2nd order pole, whose phase lag is linear in the frequency we showed and can be approximated by 650ns of time lag. In total, we have 2.2 μ s of time lag components and it explains the phase offset (see also Appendix C). In actual situation, the transfer function may have a temporal drift which decreases the accuracy of the cancellation by inverse filter. In the Appendix D, we temperature- and voltage- dependence of the transfer function, showing temporal drift is not significant enough to negatively impact the performance of the filter used here.

Fig (9) shows the measured sensitivity functions $S = y/d$ where d is the noise generated by the EOM and y is the output of the system. Two traces represent the sensitivity functions of our controller (green) and an optimized pure PI controller (blue). As we are concerned with how our controller improve the noise suppression performance against given noise spectrum d , the sensitivity function S is a natural choice because the absolute noise curve can be calculated by multiplying the sensitivity function with the noise spectrum (without feedback); i.e., the difference between the noise curve without and with the feedback is the sensitivity function. The trace without the inverse filter denoted by 'PI' clearly shows the usable bandwidth is limited by the mechanical resonance located around 30 kHz. In contrast, the PI control with our filter shown in

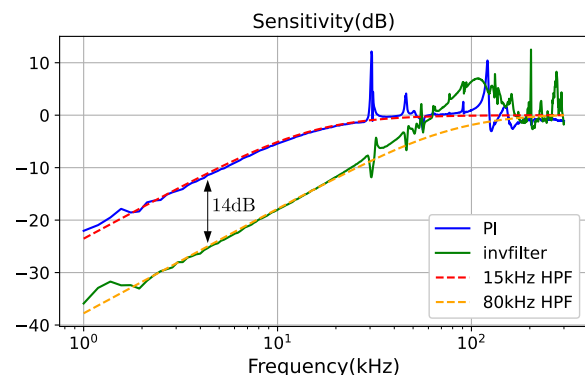


FIG. 9. Measured sensitivity function of the closed-loop interferometer system under PI control with and without filtering.

the trace denoted by 'invfilter' clearly cancels this resonance and shows 14dB of improvement in the noise suppression. A quantitative evaluation of the sensitivity function S of the integral control is possible if we model S as a first order high-pass filter $S \approx \frac{s}{s+k_i G}$, where the detail of the plant $G(s)$ are neglected. The two dotted lines in Fig(9) show the frequency response of the first order high-pass filter with cutoff frequency of 15kHz and 80kHz, which fit the sensitivity function in the low frequency region. We can see that more than five times the control bandwidth is achieved using the inverse filter. The limitation of the gain now comes from the un-cancelled resonance located around 200kHz, where mechanical resonances exist more densely than at lower frequency and a least-square method fails to capture the location of poles and zeros accurately. Further improvement may also be possible using a more accurate system identification algorithm. The disturbance of the green line at around 100kHz comes from the aforementioned 2.2 μ s non-minimum phase components. The time lag of the RedPitaya FPGA is 350ns and the remainder is attributed to the dynamics of the chosen piezo we have used for the demonstration of our controller. Here, 350ns delay corresponds to 90 degree phase lag at 700kHz so our controller can potentially achieve a few hundreds kHz of noise suppression.

VI. CONCLUSION

In this paper we have realized a high speed, digital controller for use in the high speed stabilization of an optical interferometer. This was achieved using a controller that suppresses the resonant modes of a piezo responsible for the path-length actuation. The controller was comprised of an IIR filter and PI controller. The filter we implemented is a 24 dimensional filter and the full controller had only 350ns delay. This approach presents a significant speed increase over analogous work that uses FIR filters operating with 2.6 μ s delay. Further, we also embedded in the same FPGA an accurate method of system identification required for designing the filter. The result is a complete control solution that allows for up to 24th order controllers with latency as low as 350ns. These parameters

can be optimized depending on the demand. The resulting closed-loop system was shown to have significantly greater usable bandwidth than a comparable PI controller solution which directly translated to a reduction in the interferometer phase error. The main limitation of this work comes from the un-cancelled mechanical resonance, which was not accurately estimated by simple least-square method. In the case better estimation algorithm was used and the system under control does not have non-minimum phase components, our controller will be much more effective and can achieve a broadband control up to a few hundred kHz. Future work should include exploration of more sophisticated control techniques such as LQG or H_∞ . One possibility is to optimize the filter response against the non-minimum phase component of the system. In addition, if a noise spectrum is given, such advanced controllers can suppress the total output error further than the PI-and-inverse-filter controller, with a filter response that is optimized based on the knowledge of the input. Even then, our cascaded-IIR filter implementation can be directly applicable, since any single-input single-output linear system is realized by a series of second-order filters.

VII. SUPPLEMENTARY MATERIAL

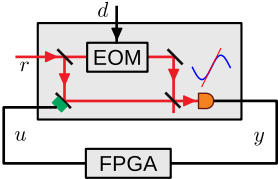
See supplementary material for the analysis of the quantization noise and truncation errors in the IIR filter, the origins of the phase offset of the identified system, and the temperature- and voltage- dependence of the transfer function of our piezo-system.

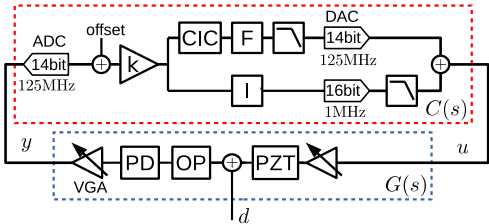
VIII. ACKNOWLEDGEMENTS

This work was partly supported by CREST (Grant No. JP-MJCR15N5), Japan Society for the Promotion of Science (JSPS) KAKENHI (grant 18H05207), UTokyo Foundation, donations from Nichia Corporation, and the Australian Research Council Centre of Excellence for Quantum Computation and Communication Technology (project CE170100012). M.O. and T.S. acknowledge financial support from ALPS.

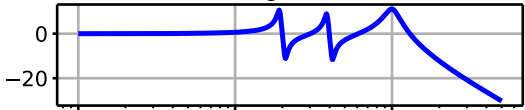
- ¹D.-H. Kim, J.-H. Han, D.-H. Kim, and I. Lee, "Vibration control of structures with interferometric sensor non-linearity," *Smart materials and structures* **13**, 92 (2003).
- ²W. Fichter, A. Schleicher, L. Szerdahelyi, S. Theil, and P. Airey, "Drag-free control system for frame dragging measurements based on cold atom interferometry," *Acta Astronautica* **57**, 788–799 (2005).
- ³L. Lublin and M. Athans, "An experimental comparison of h_2 and h_∞ designs for an interferometer testbed," in *Feedback Control, Nonlinear Systems, and Complexity* (Springer, 1995) pp. 150–172.
- ⁴A. I. Zavalin, J. Shamir, C. S. Vikram, and H. J. Caulfield, "Achieving stabilization in interferometric logic operations," *Applied optics* **45**, 360–365 (2006).

- ⁵Y. Takeno, M. Yukawa, H. Yonezawa, and A. Furusawa, "Observation of -9 db quadrature squeezing with improvement of phase stability in homodyne measurement," *Opt. Express* **15**, 4321–4327 (2007).
- ⁶J. Aasi, J. Abadie, B. Abbott, R. Abbott, T. Abbott, M. Abernathy, C. Adams, T. Adams, P. Addesso, R. Adhikari, C. Affeldt, O. Aguiar, P. Ajith, B. Allen, E. Ceron, D. Amariutei, S. Anderson, W. Anderson, K. Arai, M. Araya, C. Arceneaux, S. Ast, S. Aston, D. Atkinson, P. Aufmuth, C. Aulbert, L. Austin, B. Aylott, S. Babak, P. Baker, S. Ballmer, Y. Bao, J. Barayoga, D. Barker, B. Barr, L. Barsotti, M. Barton, I. Bartos, R. Bassiri, J. Batch, J. Bauchrowitz, B. Behnke, A. Bell, C. Bell, G. Bergmann, J. Berliner, A. Bertolini, J. Betzwieser, N. Beveridge, and P. Beyersdorf, "Enhanced sensitivity of the ligo gravitational wave detector by using squeezed states of light," *Nature Photonics* **7**, 613–619 (2013).
- ⁷H. Vahlbruch, M. Mehmet, K. Danzmann, and R. Schnabel, "Detection of 15 db squeezed states of light and their application for the absolute calibration of photoelectric quantum efficiency," *Phys. Rev. Lett.* **117**, 110801 (2016).
- ⁸T. Eberle, S. Steinlechner, J. Bauchrowitz, V. Händchen, H. Vahlbruch, M. Mehmet, H. Müller-Ebhardt, and R. Schnabel, "Quantum enhancement of the zero-area sagnac interferometer topology for gravitational wave detection," *Phys. Rev. Lett.* **104**, 251102 (2010).
- ⁹"Observation of gravitational waves from a binary black hole merger," *Phys. Rev. Lett.* **116**, 061102 (2016).
- ¹⁰H.-A. Bachor and T. C. Ralph, *A guide to experiments in quantum optics* (Wiley, 2004).
- ¹¹C. C. Gerry, "Generation of optical macroscopic quantum superposition states via state reduction with a mach-zehnder interferometer containing a kerr medium," *Physical Review A* **59**, 4095 (1999).
- ¹²P. Bertet, S. Osnaghi, A. Rauschenbeutel, G. Nogues, A. Auffeves, M. Brune, J. Raimond, and S. Haroche, "A complementarity experiment with an interferometer at the quantum–classical boundary," *Nature* **411**, 166 (2001).
- ¹³H. Yonezawa, D. Nakane, T. A. Wheatley, K. Iwasawa, S. Takeda, H. Arai, K. Ohki, K. Tsumura, D. W. Berry, T. C. Ralph, *et al.*, "Quantum-enhanced optical-phase tracking," *Science* **337**, 1514–1517 (2012).
- ¹⁴S. Yokoyama, R. Ukai, S. C. Armstrong, C. Sornphiphatphong, T. Kaji, S. Suzuki, J.-i. Yoshikawa, H. Yonezawa, N. C. Menicucci, and A. Furusawa, "Ultra-large-scale continuous-variable cluster states multiplexed in the time domain," *Nature Photonics* **7**, 982 (2013).
- ¹⁵W. P. Bowen, "Experiments towards a quantum information network with squeezed light and entanglement," (2003).
- ¹⁶Q. Zhang, W. Pan, and L. E. Cross, "Laser interferometer for the study of piezoelectric and electrostrictive strains," *Journal of Applied Physics* **63**, 2492–2496 (1988).
- ¹⁷L. C. Sinclair, J.-D. Deschênes, L. Sonderhouse, W. C. Swann, I. H. Khader, E. Baumann, N. R. Newbury, and I. Coddington, "Invited article: A compact optically coherent fiber frequency comb," *Review of Scientific Instruments* **86**, 081301 (2015).
- ¹⁸D. Goldovsky, V. Jouravsky, and A. Pe'er, "Simple and robust phase-locking of optical cavities with > 200 khz servo-bandwidth using a piezo-actuated mirror mounted in soft materials," *Optics express* **24**, 28239–28246 (2016).
- ¹⁹T. C. Briles, D. C. Yost, A. Cingöz, J. Ye, and T. R. Schibli, "Simple piezoelectric-actuated mirror with 180 khz servo bandwidth," *Opt. Express* **18**, 9739–9746 (2010).
- ²⁰V. W. C. Shum, "Dual stage suspension with pzt actuators arranged to improve actuation in suspensions of short length," (2006), uS Patent 7,023,667.
- ²¹A. Ryou and J. Simon, "Active cancellation of acoustical resonances with an fpga fir filter," *Review of Scientific Instruments* **88**, 013101 (2017).
- ²²V. Hanta and A. Prochazka, "Rational approximation of time delay," *Institute of Chemical Technology in Prague. Department of computing and control engineering. Technická* **5**, 28 (2009).
- ²³L. Ljung, "System identification," *Wiley Encyclopedia of Electrical and Electronics Engineering* (2001).
- ²⁴C. L. Phillips and J. H. Troy Nagle, *Digital Control System Analysis and Design* (Prentice-Hall, 1985).
- ²⁵H. J. Siegel, "A model of simd machines and a comparison of various interconnection networks," *IEEE Transactions on Computers* , 907–917 (1979).

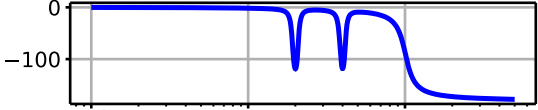




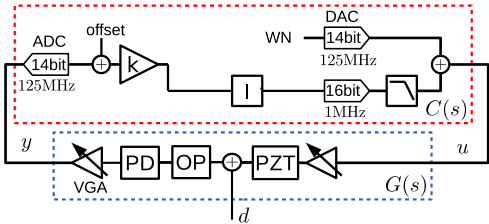
PZT gain (dB)



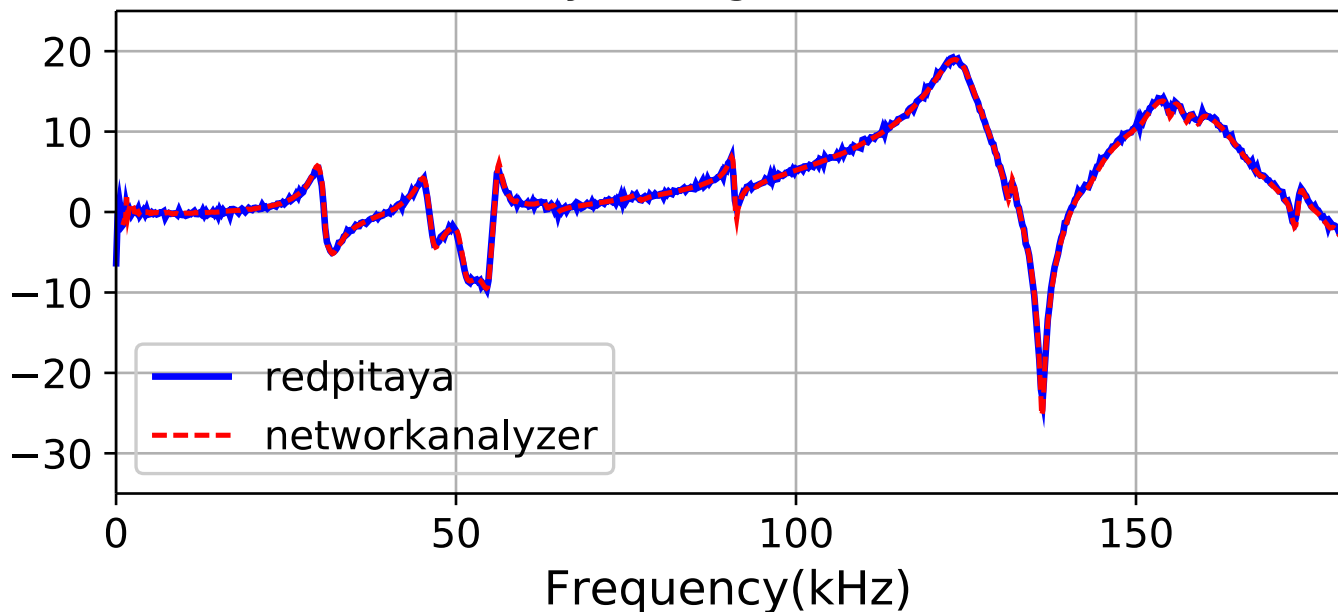
PZT phase (deg)



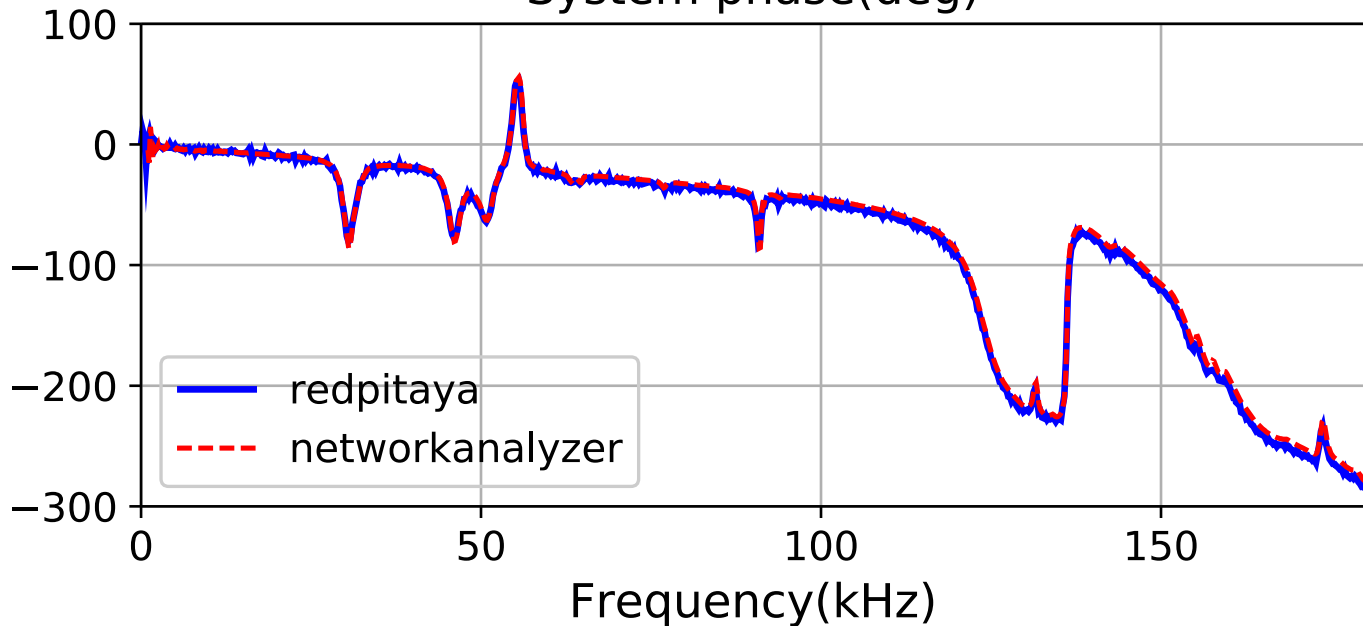
Frequency (Hz)

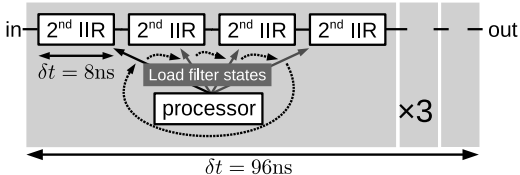


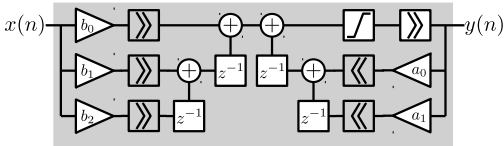
System gain(dB)



System phase(deg)







round to int/frac

Clipping int to

 : 0/36

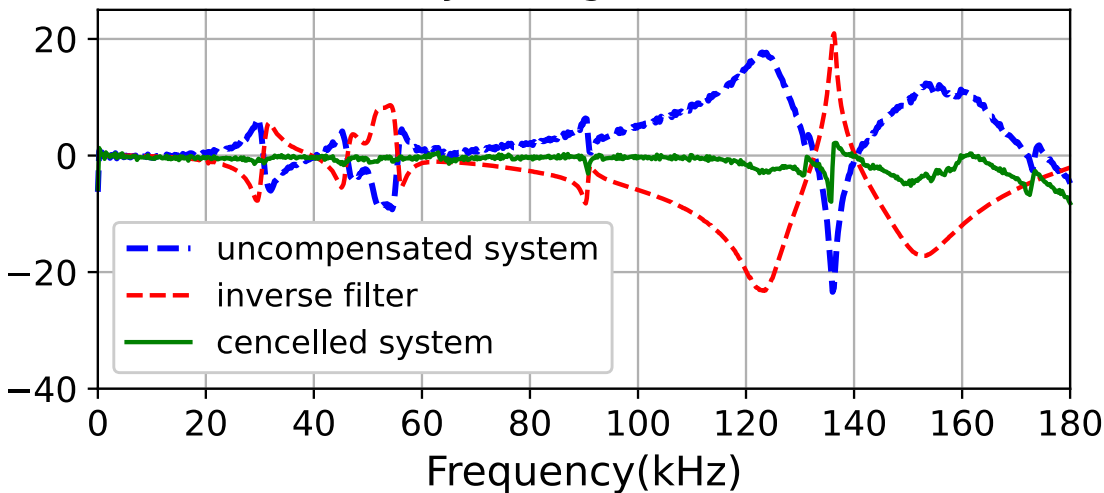
 : 6/36

 : 0/25

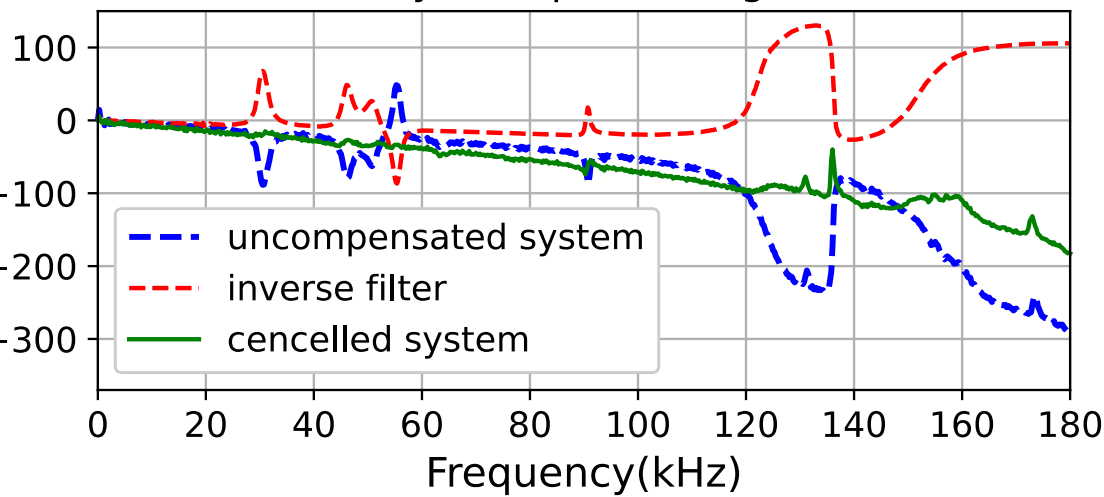
multiple by int/frac

 : 3/22

System gain(dB)



System phase(deg)



Sensitivity(dB)

